INTERNATIONAL JOURNAL OF HYDROGEN ENERGY 37 (2012) 17921–17927

Available online at www.sciencedirect.com

SciVerse ScienceDirect

journal homepage: www.elsevier.com/locate/he

In situ facile synthesis of ruthenium nanocluster catalyst supported on carbon black for hydrogen generation from the hydrolysis of ammonia-borane

Hongyan Liang [a], *Guozhu Chen* [a], *Stefano Desinan* [a], *Renzo Rosei* [b,c], *Federico Rosei* [a,c,d], *Dongling Ma* [a,*]

[a] *Institut National de la Recherche Scientifique (INRS), Énergie, Matériaux et Télécommunications, Université du Québec, 1650 Boulevard Lionel-Boulet, Varennes, QC J3X 1S2, Canada*

[b] *Physics Department, Trieste University, Via Valerio 2, I-34127, Italy*

[c] *Italy–Quebec Joint Laboratory in Nanostructured Materials for Energy, Catalysis and Biomedical Applications, Italy*

[d] *Centre for Self-Assembled Chemical Structures, McGill University, Montreal, QC H3A 2K6, Canada*

ARTICLE INFO

Article history:
Received 28 June 2012
Received in revised form
27 August 2012
Accepted 4 September 2012
Available online 3 October 2012

Keywords:
Ruthenium nanoclusters
In situ synthesis
Ammonia-borane catalytic hydrolysis
Hydrogen generation

ABSTRACT

Ligand-free Ru nanoclusters supported on carbon black have been synthesized in situ for the first time from the reduction of $RuCl_3$ by ammonia-borane concomitantly with its hydrolysis process at room temperature, and their catalytic activity has been investigated. Well dispersed Ru nanoclusters (~1.7 nm) are stabilized and immobilized by carbon black. Due to the small size and the absence of ligands on the surface, the Ru catalysts exhibit high catalytic activity, which is partly retained after 5 reaction cycles. A kinetic study shows that the catalytic hydrolysis of ammonia-borane is first order with respect to Ru catalyst concentration; the turnover frequency is 429.5 mol H_2 min^{-1} mol^{-1} Ru. The activation energy for the hydrolysis of ammonia-borane in the presence of Ru/C catalysts has been measured to be 34.81 ± 0.12 kJ mol^{-1}, which is smaller than most of the values reported for other catalysts, including those based on Ru, for the same reaction.

1. Introduction

Hydrogen is regarded as a clean energy carrier due to its high efficiency and power density, and its limited environmental impact [1]. One of the key issues in studies on hydrogen as an energy carrier is to develop suitable hydrogen storage materials, with the desirable properties of high hydrogen storage capacity and controllable release rate, air stability, non-flammability, and low toxicity [2,3]. Among these, ammonia-borane (NH_3BH_3, AB) has been identified as an attractive candidate, because of its high hydrogen content (19.6%), its stability under ordinary storage conditions, and its environmental benignancy [1,4]. The release of hydrogen from AB can be obtained through pyrolysis in the solid state, and hydrolysis or methanolysis in solution [4–9]. The pyrolysis process requires high temperature and power consumption [8]. In contrast, catalytic hydrolysis or methanolysis are more promising ways. The stoichiometric amount of hydrogen (H_2/AB = 3.0) could be released from hydrolysis process under mild conditions [9]. However, this process occurs at appreciable rate only in the presence of a suitable catalyst, therefore, catalysts are the dominant factor in this process.

* *Corresponding author*. Tel.: +1 514 228 6920; fax: +1 450 929 8102.
E-mail address: ma@emt.inrs.ca (D. Ma).

0360-3199/$ – see front matter
http://dx.doi.org/10.1016/j.ijhydene.2012.09.026

Developing efficient and economical catalysts enhancing the hydrolysis rate under moderate conditions is crucial. So far, numerous monometallic catalysts, such as noble metals Rh [10–12], Pd [10,13], Ru [10,13–17] and Pt [10] and non-noble metals Fe [18,19], Ni [17,18,20,21], Co [11,18,21] have been evaluated. Besides monometallic catalysts, bimetallic ones, such as core/shell structured $Ni_{1-x}@Pt_x$ [22] and Ni@Ru [23] nanoparticles and alloyed RuNi [17], CoPt [24], RuCo and RuCu nanoparticles [25], and trimetallic ones, such as Co–Ni–P [26] and Cu@FeNi [27], were also tested for AB hydrolysis. Ru nanoparticles have been identified as one of the most effective ones.

To be active in the hydrolysis of AB, catalysts are required to have small size (<10 nm), which causes an increase in the surface area and thus the number of active sites [24]. For this purpose, ligands are often used to control the size of catalysts and prevent their agglomeration. For example, poly (4-styrenesulfonic acid-co-maleic acid) stabilized ruthenium(0) and palladium(0) nanoclusters [13] and laurate-stabilized ruthenium(0) nanoclusters [14] have been investigated for hydrogen generation from the hydrolysis of AB. In previous work, we reported new core–shell structured Ni@Ru [23] and hollow Ru [28] nanoparticles supported on carbon black as a catalytic system for the hydrolysis of AB, where oleic acid and oleylamine act as surface ligands for the bimetallic nanoparticles. Although high catalytic activity was observed in all these cases, the presence of surface ligands in general leads to the decrease of catalytic activity, since a fraction of surface active sites are blocked [14]. Impregnation is a well established approach for acquiring ligand-free, small metal nanoparticles on various supports. However, their size distribution is difficult to control. Furthermore, the sensitivity of metal nanoparticles to air exposure also needs to be considered, since their catalytic activity may decrease upon oxidation when they are handled and transferred in liquid phase [9,10].

In situ synthesis of catalyst is a method that has been devoted a lot of attention recently [7]. Metal cations are reduced by certain chemical to their metallic state, which without any purification directly acts as catalysts to catalyze chemical reactions involving the same chemical. This process is simple and no further treatment is necessary, thus the loss of catalyst or its oxidation during the transfer process can be avoided. Aiming to develop high-efficiency and economical catalysts, we decided to further explore this in situ method for synthesizing Ru nanoclusters that have large surface area. Herein, we report the in situ synthesis of ultra-small, ligand-free Ru nanoclusters, stabilized and supported by Ketjen carbon black (Ru/C), through reduction of $RuCl_3 \cdot nH_2O$ during the hydrolysis process of AB. Ketjen carbon black was chosen as a support because it has been reported as a very good support for catalysts in the AB hydrolysis reaction [17,20,23,28]. The basic concept of this approach is to take advantage of the high surface area of carbon black and the reducibility of Ru^{3+} by AB to obtain highly dispersed and stable Ru nanoclusters. Our approach avoids possible drawbacks due to the presence of ligands, problems related to uncontrolled broad size distribution of catalyst particles, and mass loss or metal oxidation during purification and transferring processes. As a result, high activity catalysts were obtained. A kinetic investigation of the reaction was also carried out by varying the $RuCl_3 \cdot nH_2O$ concentration and temperature.

2. Experimental

2.1. Materials

Ruthenium (III) chloride hydrate ($RuCl_3 \cdot nH_2O$, 99.98%), and AB (NH_3BH_3, 90%) were purchased from Sigma–Aldrich Inc. Electroconductive carbon black Ketjenblack EC-300J was obtained from AkzoNobel Company. All chemicals were used as obtained. Deionized water with a specific resistance of 18.2 MΩ was distilled by water purification system (Milli Q-pure WS) and used in all operations.

2.2. In situ synthesis of Ru/C catalysts

Ru/C catalysts were synthesized in situ by reducing the $RuCl_3 \cdot nH_2O$ using AB in aqueous solution. In a typical synthesis, 1 mL of 8.5 mM $RuCl_3 \cdot nH_2O$ solution was diluted in 7 mL of deionized water and 10 mg of carbon black were added into this solution. Ultrasonication was required to get a uniform dispersion. The mixture was stirred for further 12 h at room temperature. Then AB (2 mL, 1 M in water) was added into this mixture to start the reduction of $RuCl_3 \cdot nH_2O$ and AB catalytic hydrolysis. A water bath was used to control the temperature of the reaction solution. The $RuCl_3 \cdot nH_2O$ was firstly reduced by AB and then used as the catalyst for hydrolysis of AB. The Ru/C suspension was vigorously stirred with a magnetic stirrer during all the reaction. For comparison, a Ru catalyst without support was also prepared by the same procedure as described above.

2.3. Characterization

Ru/C catalysts were purified from the reaction solution by centrifugation for further characterization. The morphology of Ru/C catalysts was characterized using a JEOL 2100F transmission electron microscopy (TEM). The average particle size of the Ru nanoclusters was measured from TEM micrographs. The presence of Ru on the Ru/C catalysts was confirmed by energy dispersive X-ray spectrometry (EDX). The X-ray diffraction (XRD) study of Ru/C catalysts was carried out with a Philips X'pert diffractometer using Cu $K\alpha$ radiation source ($\lambda = 0.15418$ nm). X-ray photoelectron spectrometry (XPS) was performed on a VG Escalab 220i-XL equipped with an Al $K\alpha$ source. Purified Ru/C catalysts and dried $RuCl_3$/C mixtures were used for XPS analysis. Neutron activation analysis (NAA) at SLOWPOKE nuclear reactor (École Polytechnique de Montréal, Montréal, Canada) was conducted to determine the elemental composition of solid samples and solutions. As prepared $RuCl_3$ solution, $RuCl_3$/C solution (after mixing $RuCl_3$ and C for 12 h), Ru/C-1st cycle and Ru/C-5th cycle solutions were filtered and 1 mL of the filtrates were sent to the NAA analysis. For comparison of the element loss before and after filtering, an unfiltered solution of $RuCl_3$ alone was also tested. The filtered solution of every sample (1 mL) and an unfiltered $RuCl_3$ solution (1 mL) were analyzed by NAA. Fourier transform infrared spectroscopy (FT–IR) of pure

carbon black was taken from a Thermo Nicolet 6700 infrared spectrometer with resolution of 0.5 cm^{-1}. The Brunauer–Emmett–Teller (BET) method was used for evaluation of the surface area and pore size of carbon black. N_2 physisorption experiments were performed at 77 K on a 3100 surface area analyzer (Beckman Coulter).

2.4. Catalytic hydrolysis of AB

The catalytic activity of Ru/C in the hydrolysis of AB was determined by measuring the rate of hydrogen generation. The volume of gas was monitored by recording the displacement of water level in an inverted and graduated water-filled burette (Aldrich® graduated burette). Through following the progress of an individual hydrolysis reaction in volumetric measurement at constant time interval, the rate of hydrogen generation can be measured. The turnover frequency (TOF) (mol $H_2 \cdot min^{-1}$ mol^{-1} Ru) of AB hydrolysis was estimated from the linear portion of the volume/time plot. Sets of experiments with different concentration of Ru (0.21, 0.51, 0.85, 1.27, 1.7 mM) were performed at room temperature (25 ± 1 °C) while the AB concentration was kept the same (200 mM) to determine the rate law of the catalytic hydrolysis of AB. Temperature was varied at 14 ± 1 °C, 25 ± 1 °C, 33 ± 1 °C and 37 ± 1 °C while the concentration of Ru (0.85 mM) and AB (200 mM) were kept constant to obtain the activation energy (E_a). A low concentration of AB and Ru were used to restrict the reaction rate in a measurable range and minimize the heat generation affecting the hydrolysis process. For durability tests, the reactions were repeated 5 times. The 1st cycle refers to the reduction of Ru^{3+} by AB and simultaneous AB hydrolysis reaction. For the 2nd to 5th cycles, as the previous hydrolysis was completed, 2 mL of the transparent supernatant solution were removed from reactor and then an equivalent volume (2 mL) of AB (1 M) solution was added to start the next cycle.

3. Results and discussion

3.1. Characterization of Ru nanoclusters supported on carbon black

The morphology and size of Ru were investigated by TEM. It is known that carbon black tends to form chainlike aggregates as shown in Fig. 1A [10]. Ru nanoclusters with an average diameter of ~1.7 nm (Fig. S1) were uniformly dispersed on the carbon black support. No obvious aggregation was found in the TEM images, indicating that most of the nanoclusters are individually adhering to carbon black in water, rather than forming aggregates, as is the case in the absence of a stabilizing support (in this case, the average diameter of Ru nanoclusters which are not in aggregation is 2.8 ± 0.7 nm; the size of Ru nanoclusters in aggregation cannot be unambiguously identified, Fig. S2). The presence of Ru on the carbon black support was further confirmed by EDX as shown in Fig. 1B. XRD pattern of Ru/C catalysts is shown in Fig. 1C. The peak at 2θ ~24° is associated with the carbon black while the strong diffraction peak at 2θ ~44° is attributed to the (101) plane of hexagonal close-packed phase of metallic Ru with a d-value of 2.06 Å [28,29]. The broad Ru peak suggests that the size of particles is quite small at the nanoscale, which is consistent with the particle size distribution (Fig. S1) from our TEM analysis [28,29].

XPS was used to investigate the chemical valence state of Ru before and after reduction by AB. The Ru $3d_{3/2}$ peak around 285 eV overlaps with the C 1s peak, therefore, the Ru $3p_{3/2}$ peak was chosen for comparison instead. After mixing $RuCl_3$ and carbon black for 12 h, there is no significant change of intensity of the peak centered at 463.7 eV, which is assigned to the Ru $3p_{3/2}$ in $RuCl_3$ (Fig. 2). It seems that there is no special interaction between the carbon black and Ru^{3+}. This is consistent with the negligible change of Ru element concentration in the $RuCl_3$ solution, quantified by NAA before (76.9 ppm) and after (73.7 ppm) mixing with carbon black (Table 1). After the $RuCl_3$ was reduced by AB, the Ru $3p_{3/2}$ peak fits well to two deconvoluted peaks at 462.2 and 465.4 eV, assigned to the Ru(0) $3p_{3/2}$ and Ru(IV) $3p_{3/2}$ [14,30] respectively. The Ru(0) $3p_{3/2}$ confirms the formation of Ru nanoclusters with the reduction by AB. Ru (IV) oxide present on the surface of Ru likely forms during the sample preparation process for XPS measurements [30].

To understand the interaction between the Ru nanoclusters and C, an investigation of the carbon black surface is necessary. The nature of the surface groups of carbon black were verified by FT–IR characterization as shown in Fig. 3. The peak centered at 1575 cm^{-1} is due to the vibration of C–O groups and the weak and narrow peak located at 3736 cm^{-1} is due to the vibration of O–H groups, which indicates that the carbon black has –OH groups on the surface, consistent with the material specifications provided by the manufacturing company. In fact, after the $RuCl_3$ was mixed with the carbon black for 12 h, most of the precursors were still free in solution, instead of attaching onto the surface of the support, based on the high Ru concentration in solution (Table 1).

Although we expect Ru cations easily bind to the –OH groups on carbon black (the pH of 10 mM $RuCl_3 \cdot nH_2O$ is 2.75), this does not seem to be the case. Based on the BET analysis, the carbon black Ketjenblack EC-300J has micropores (<2 nm) and a very large surface area of 800 m^2 g^{-1} (Fig. S3). Therefore, we propose that after adding the AB, the newly formed Ru nanoclusters are highly unstable due to their small size and ligand-free surface. These nanoclusters are prone to aggregation to release their surface energy in the absence of any supports or protecting molecules (or ions). In the presence of carbon black, these Ru nanoclusters are almost totally adsorbed on its surface because of its high surface area. Thus, carbon black effectively stabilizes Ru nanoclusters and prevents them from agglomerating, based on the TEM observation and NAA analysis mentioned above. Although there is no strong chemical interaction between carbon black and Ru, the Ru nanoclusters do not detach from the support under the vigorous stirring in the reaction. The large number of small pores in carbon black quite possibly confines Ru nanoclusters' mobility and immobilizes them, dramatically decreasing Ru concentration in the solution (<5 ppm, Table 1). The reducing reactions were also performed with different $RuCl_3$ concentration and different reaction temperature. It was found that all the Ru nanoclusters on carbon black support exhibit very small size (~1.7 nm) with even distribution (Fig. S1) regardless of the synthesis conditions. This offers us a chance to evaluate the catalytic activity of Ru/C catalysts at different Ru concentration and temperature.

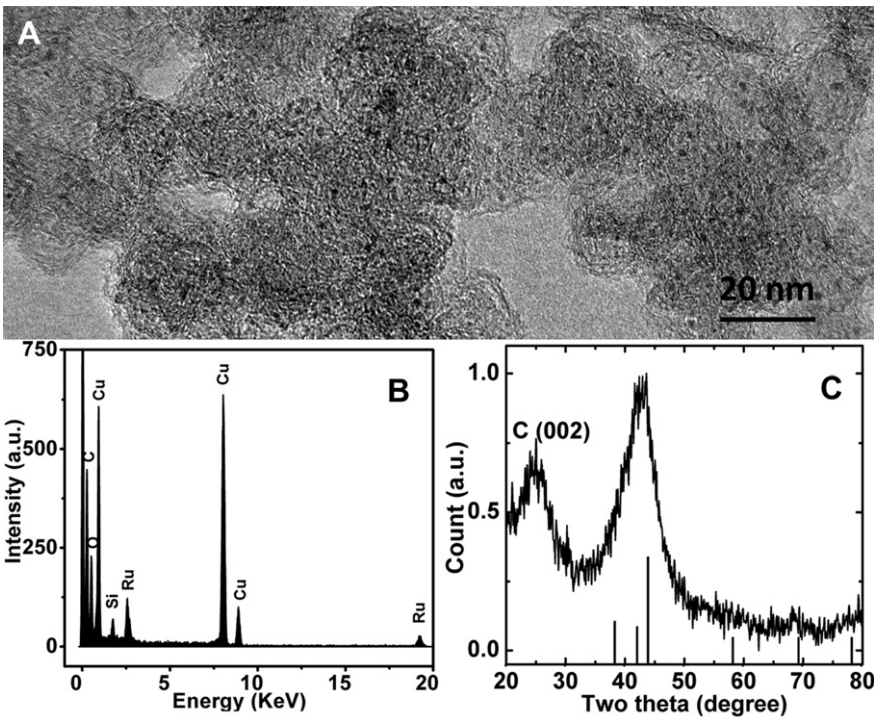

Fig. 1 – (A) TEM image of the Ru nanoclusters on the carbon black support. (B) EDX and (C) XRD pattern of the Ru/C catalysts.

3.2. *Kinetic study of hydrolysis of AB catalyzed by Ru nanoclusters on the carbon black*

The in situ synthesized Ru nanoclusters on the carbon black can directly serve as catalysts for AB hydrolysis. The volume of hydrogen gas was measured by recording the displacement of water level in an inverted and graduated water-filled burette. The activity of Ru/C catalysts can be easily estimated from the time for the complete hydrolysis of an injected amount of AB. In our case, the molar ratio of AB to $RuCl_3$ is higher than 100, therefore, the volume of hydrogen generated by $RuCl_3$ before it is rapidly reduced to form Ru(0) can be ignored [7]. Fig. 4 shows the plots of the volume of hydrogen generated versus time during the catalytic hydrolysis with different initial $RuCl_3$ concentration at 25 ± 1 °C. It was found that the H_2 evolution is very fast and nearly linear reaction time. The hydrogen generation started without an obvious induction period and continued until the complete hydrolysis of AB.

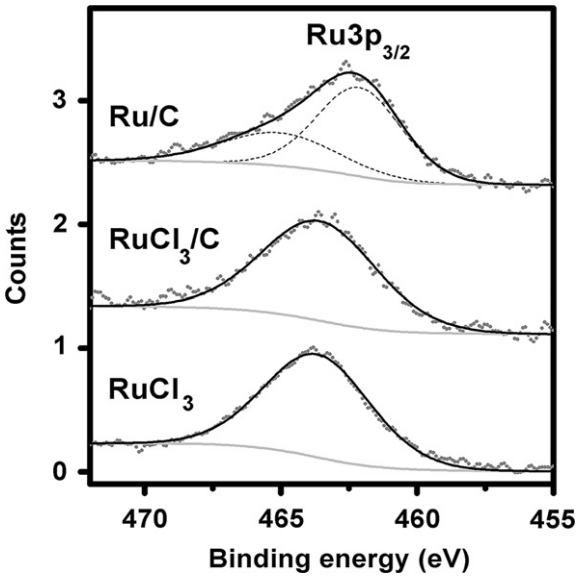

Fig. 2 – High resolution Ru 3p XPS spectra of filtered solutions of $RuCl_3$, $RuCl_3$/C (after mixing $RuCl_3$ with carbon black for 12 h), and Ru/C (after reducing $RuCl_3$ by AB). The gray dots represent the experimental data. The black dash and gray solid lines are fitting and background curves, respectively. In the top spectrum, the black solid line is the sum of two black dash fitting curves.

Considering the purity of as-received $RuCl_3$, the actual concentration of Ru catalysts in the reaction solution was directly measured by NAA. Sets of experiments with different concentration of Ru were performed at constant AB concentration (200 mM) to determine the rate law of the catalytic hydrolysis of AB. With an increase of Ru concentration, the reaction time decreased from 570 s ([Ru] = 0.21 mM) to 65 s ([Ru] = 1.7 mM) for the complete hydrogen release. The TOF of AB hydrolysis was estimated from the linear portion of the plot. Under our reaction conditions, the activity in terms of TOF at 25 ± 1 °C is 429.5 mol H_2 min^{-1} mol^{-1} Ru. This indicates that the Ru/C catalysts are among the most active catalysts compared with what has been reported on the performance of various Ru-based and other catalysts for the hydrolysis of AB at room temperature [10,13–16]. Both the high surface area of the non-aggregated, small nanoclusters and their ligand-free surface directly contribute to enhancing the catalytic activity due to the presence of more available surface sites. The plot of hydrogen generation rate versus Ru concentration in logarithmic scale is inserted in Fig. 4; it follows a linear relationship. The slope of the line is 0.93, which is close to 1, indicating

Table 1 – NAA elemental analysis of the initial solution of $RuCl_3$, filtered initial solution of $RuCl_3$, $RuCl_3$/C mixture and Ru/C catalysts after a different number of reaction cycles.

Sample	Ru (ppm)
$RuCl_3$	86.1
Filtered $RuCl_3$	76.9
$RuCl_3$/C	73.7
RuC 1st cycle	<5
RuC 5th cycle	<3

that the hydrolysis reaction is first order with respect to the catalyst concentration.

Fig. 5 shows the plots of volume of hydrogen generated versus time in the hydrolysis of 200 mM AB catalyzed by Ru/C catalysts ([Ru] = 0.85 mM) at various temperatures in the range 14–37 °C to determine the activation energy. Increasing the temperature gives a higher reaction rate. When the temperature is set at 37 °C, the reaction ends in 60 s, while at the lowest temperature (14 °C) investigated herein the completion of the hydrogen release requires 390 s. In addition, at 14 °C an induction period of less than 70 s was observed due to the slow activation of the catalysts. The reaction rate constant *k* for the hydrolysis of AB was estimated from the linear portion of the plots in Fig. 5 at different temperatures. The corresponding Arrhenius plot (ln *k* *vs* 1/T) is shown in the inset of Fig. 5. From the slope of the straight line, the activation energy (*Ea*) for the hydrolysis of AB was estimated. Although the *Ea* value of 34.81 ± 0.12 kJ mol^{-1} in our experiment is higher than that (Ea = 23 kJ mol^{-1}) reported for Ru/γ-Al_2O_3 [10], it is lower than that of most other Ru catalysts: 54 ± 2 kJ mol^{-1} for poly(4-styrenesulfonic acid-co-maleic acid) stabilized Ru nanoclusters [13]; 47 ± 2 kJ mol^{-1} for laurate-stabilized Ru nanoclusters [14]; 76 ± 0.1 kJ mol^{-1} for carbon supported commercial Ru [15]; 67 kJ mol^{-1} for Ru and RuO_2 supported over γ-Al_2O_3 [16]. This further proves that the in situ synthesized Ru/C catalysts are very promising candidates for the hydrolysis of AB.

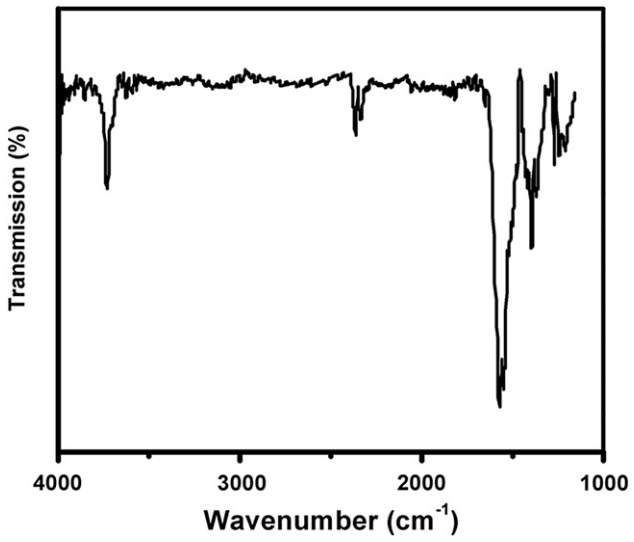

Fig. 3 – FT–IR of carbon black.

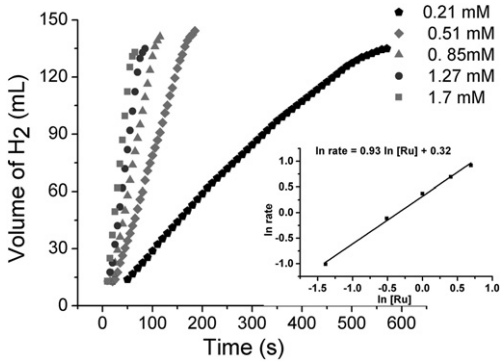

Fig. 4 – The volume of hydrogen versus time graph for the Ru/C catalytic hydrolysis of AB for different Ru concentration at 25 ± 1 °C. The inset shows the plot of hydrogen generation rate versus the concentration of Ru (both in logarithmic scale).

3.3. *Catalyst durability study of hydrolysis of AB catalyzed by Ru nanoclusters on the carbon black*

In general, reduced catalyst reactivity upon repeated use is a big drawback for application. Recyclability tests of Ru/C catalysts were performed on 0.85 mM Ru concentration. It showed that the as-prepared Ru/C catalysts still exhibited certain catalytic activity after multiple cycles of reaction (Fig. 6). After five cycles, the Ru/C catalysts retain 43.1% of the initial catalytic activity. The decrease of catalytic activity could be easily attributed to the loss of Ru from the surface of carbon black. If the Ru nanoclusters detach from the support, they would aggregate in solution and their catalytic activity would decrease. To test this hypothesis, we measured the Ru concentration in the solution after removing the carbon black along with attached Ru by filtration. As shown in Table 1, the concentration of Ru in the filtered solution is negligible along the 5 cycles (3–5 ppm). The low concentration of Ru in the solution shows that most of Ru nanoclusters are still attached on the surface of carbon black after several cycles, instead of dispersing into the solution. TEM imaging of Ru/C catalysts

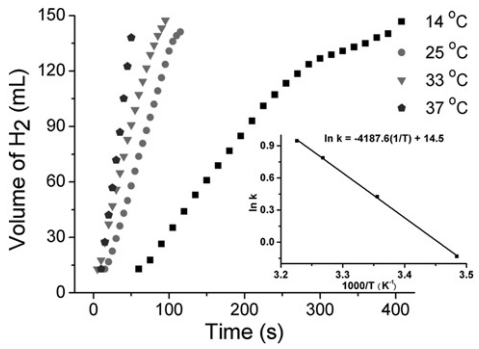

Fig. 5 – The volume of hydrogen versus time graph for the Ru/C catalytic hydrolysis of AB at different temperatures, [Ru] = 0.85 mM, [AB] = 200 mM. The inset shows the Arrhenius plot (ln *k* versus the reciprocal absolute temperature, 1/*T* (K^{-1})).

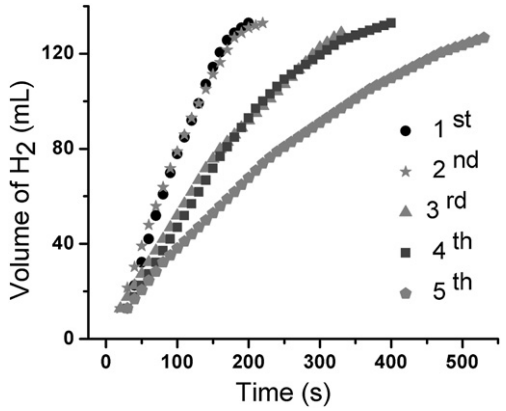

Fig. 6 – Graph of hydrogen versus time for the Ru/C catalytic hydrolysis of AB from 1st to 5th cycles at 22 ± 1 °C, [Ru] = 0.85 mM, and [AB] = 200 mM.

(shown in Fig. S1) proves that there is no significant change in the particles' size or morphology after five cycles. This means that there is no obvious aggregation of Ru nanoclusters. These results show that the carbon black can stabilize and immobilize Ru nanoclusters at least for five cycles. Therefore, the observed decrease in catalytic activity in consecutive cycles should not be attributed to the detachment of Ru from the carbon black or aggregation of Ru nanoclusters on the support. The reason for the loss of activity in the hydrolysis of AB may be due to the increasing concentration of reaction product in solution. The metaborate and Cl^- ions from $RuCl_3$ precursor could adsorb on Ru nanoclusters' surface, capping their active sites [7]. In addition, the increase in viscosity of the solution after many runs might hinder the diffusion of AB, impeding the collision between AB and Ru nanoclusters, thus decreasing the catalytic activity correspondingly [7]. Further investigations on the "re-generation" of the catalytic system will be performed in order to maintain the high catalytic activity of these tiny Ru nanoparticles in the long run.

4. Conclusion

In summary, we demonstrated that ligand-free Ru nanoclusters supported by carbon black can be easily synthesized in situ by reduction of $RuCl_3$ concomitantly with the hydrolysis process of AB at room temperature. Ru/C catalysts having an average size of ~1.7 nm exhibit high activity (TOF = 429.5 mol H_2 min^{-1} mol^{-1} Ru) and low activation energy ($Ea = 34.81 \pm 0.12$ kJ mol^{-1}). In the view of a portable application, a high TOF could be an asset in the miniaturization of an on-board hydrogen storage system. Ru/C catalysts also show fair stability during the recycling tests and 43.1% of the initial activity is retained after 5 cycles.

Acknowledgments

We acknowledge Dr. Lefevre Michel for the BET characterization. Financial support from the Merit Scholarship Program for Foreign Students from the Ministère de l'Éducation, du Loisir et du Sport du Québec is greatly appreciated. We also thank the Natural Sciences and Engineering Research Council of Canada (NSERC) and Agence de l'efficacité énergétique for their financial support. Federico Rosei is grateful to the Canada Research Chairs Program for partial salary support.

Appendix A. Supplementary data

Supplementary data related to this article can be found at http://dx.doi.org/10.1016/j.ijhydene.2012.09.026.

REFERENCES

[1] Schlapbach L, Züttel A. Hydrogen-storage materials for mobile applications. Nature 2001;414:353–8.
[2] Eberle U, Felderhoff M, Schüth F. Chemical and physical solutions for hydrogen storage. Angew Chem Int Ed 2009;48:6608–30.
[3] Yang J, Sudik A, Wolverton C, Siegel DJ. High capacity hydrogen storage materials: attributes for automotive applications and techniques for materials discovery. Chem Soc Rev 2010;39:656–75.
[4] Grochala W, Edwards PP. Thermal decomposition noninterstitial hydrides for the storage and production hydrogen. Chem Rev 2004;104:1283–316.
[5] Mohajeri N, Raissi A, Adebiyi O. Hydrolytic cleavage of ammonia-borane complex for hydrogen production. J Power Sources 2007;167:482–5.
[6] Hamilton CW, Baker RT, Staubitz A, Manners I. B-N compounds for chemical hydrogen storage. Chem Soc Rev 2009;38:279–93.
[7] Erdoğan H, Metin Ö, Özkar S. In situ-generated PVP-stabilized palladium(0) nanocluster catalyst in hydrogen generation from the methanolysis of ammonia-borane. Phys Chem Chem Phys 2009;11:10519–25.
[8] Staubitz A, Robertson APM, Manners I. Ammonia-borane and related compounds as dihydrogen sources. Chem Rev 2010;110:4079–124.
[9] Jiang H, Xu Q. Catalytic hydrolysis of ammonia borane for chemical hydrogen storage. Catal Today 2011;170:56–63.
[10] Chandra M, Xu Q. Room temperature hydrogen generation from aqueous ammonia-borane using noble metal nanoclusters as highly active catalysts. J Power Sources 2007;168:135–42.
[11] Clark TJ, Whittell GR, Manners I. Highly efficient colloidal cobalt- and rhodium-catalyzed hydrolysis of H_3NBH_3 in air. Inorg Chem 2007;46:7522–7.
[12] Zahmakiran M, Özkar S. Zeolite framework stabilized rhodium(0) nanoclusters catalyst for the hydrolysis of ammonia-borane in air: outstanding catalytic activity, reusability and lifetime. Appl Catal B 2009;89:104–10.
[13] Metin Ö, Sahin S, Özkar S. Water-soluble poly (4-styrenesulfonic acid-co-maleic acid) stabilized ruthenium(0) and palladium(0) nanoclusters as highlyactive catalysts in hydrogen generation from the hydrolysis of ammonia-borane. Int J Hydrogen Energy 2009;34:6304–13.
[14] Durap F, Zahmakıran M, Özkar S. Water soluble laurate-stabilized ruthenium(0) nanoclusters catalyst for hydrogen generation from the hydrolysis of ammonia-borane: high activity and long lifetime. Int J Hydrogen Energy 2009;34:7223–30.
[15] Basu S, Brockman A, Gagare P, Zhen Y, Ramachandran PV, Delgass WN. Chemical kinetics of Ru-catalyzed ammonia borane hydrolysis. J Power Sources 2009;188:238–43.

[16] Rachiero GP, Demirci UB, Miele P. Facile synthesis by polyol method of a ruthenium catalyst supported on γ-Al_2O_3 for hydrolytic dehydrogenation of ammonia borane. Catal Today 2011;170:85–92.
[17] Chen GZ, Desinan S, Rosei R, Rosei F, Ma DL. Synthesis of Ni-Ru alloy nanoparticles and their high catalytic activity in dehydrogenation of ammonia borane. Chem Eur J 2012;18: 7925–30.
[18] Xu Q, Chandra M. Catalytic activities of non-noble metals for hydrogen generation from aqueous ammonia-borane at room temperature. J Power Sources 2006;163:364–70.
[19] Yan JM, Zhang XB, Han S, Shioyama H, Xu Q. Iron nanoparticle-catalyzed hydrolytic dehydrogenation of ammonia borane for chemical hydrogen storage. Angew Chem Int Ed 2008;47:2287–9.
[20] Metin Ö, Mazumder V, Özkar S, Sun SH. Monodisperse nickel nanoparticles and their catalysis in hydrolytic dehydrogenation of ammonia borane. J Am Chem Soc 2010; 132:1468–9.
[21] Metin Ö, Özkar S. Water soluble nickel(0) and cobalt(0) nanoclusters stabilized by poly(4-styrenesulfonic acid-co-maleic acid): highly active, durable and cost effective catalysts in hydrogen generation from the hydrolysis of ammonia borane. Int J Hydrogen Energy 2011;36: 1424–32.
[22] Yang XJ, Cheng FY, Liang J, Tao ZL, Chen J. Carbon-supported Ni(1-x)@Pt(x) (x = 0.32, 0.43, 0.60, 0.67, and 0.80) core-shell nanoparticles as catalysts for hydrogen generation from hydrolysis of ammonia borane. Int J Hydrogen Energy 2011; 36:1984–90.
[23] Chen GZ, Desinan S, Nechache R, Rosei R, Rosei F, Ma DL. Bifunctional catalytic/magnetic Ni@Ru core–shell nanoparticles. Chem Commun 2011;47:6308–10.
[24] Sun D, Mazumder V, Metin Ö, Sun S. Catalytic hydrolysis of ammonia borane via cobalt palladium nanoparticles. ACS Nano 2011;5:6458–64.
[25] Rachiero GP, Demirci UB, Miele P. Bimetallic RuCo and RuCu catalysts supported on γ-Al_2O_3. A comparative study of their activity in hydrolysis of ammonia-borane. Int J Hydrogen Energy 2011;36:7051–65.
[26] Rakap M, Kalu EE, Özkar S. Hydrogen generation from the hydrolysis of ammonia borane using cobalt-nickel-phosphorus (Co–Ni–P) catalyst supported on Pd-activated TiO_2 by electroless deposition. Int J Hydrogen Energy 2011;36:254–61.
[27] Wang HL, Yan JM, Wang ZL, Jiang Q. One-step synthesis of Cu@FeNi core-shell nanoparticles: highly active catalyst for hydrolytic dehydrogenation of ammonia borane. Int J Hydrogen Energy 2012;37:10229–35.
[28] Chen GZ, Desinan S, Rosei R, Rosei F, Ma DL. Hollow ruthenium nanoparticles with small dimensions derived from Ni@Ru core@shell structure: synthesis and enhanced catalytic dehydrogenation of ammonia borane. Chem Commun 2012;48:8009–11.
[29] Corain B, Schmid G, Toshima N. Metal nanoclusters in catalysis and materials science: the issue of size control. Netherlands: Elsevier; 2007. ch. 7.
[30] Park K-W, Choi J-H, Kwon B-K, Lee S-A, Sung Y-E. Chemical and electronic effects of Ni in Pt/Ni and Pt/Ru/Ni alloy nanoparticles in methanol electrooxidation. J Phys Chem B 2002;106:1869–77.